Materials Letters 15 (1993) 370–375
North-Holland

MATERIALS LETTERS

Some methods for kinetic studies of non-isothermal crystallization in $Sn_{0.08}As_{0.26}Se_{0.66}$ alloy

C. Wagner, P. Villares, J. Vázquez and R. Jiménez-Garay
Facultad de Ciencias, Universidad de Cádiz, Puerto Real (Cádiz), Spain

Received 21 September 1992; in final form 13 October 1992

The crystallization reaction of $Sn_{0.08}As_{0.26}Se_{0.66}$ chalcogenide glass was taken as a reference for determining the kinetic parameters (activation energy, E, reaction order, n, and frequency factor, K_0) which describe the said reaction by differential scanning calorimetry and using non-isothermal techniques. Two sets of kinetic parameters have been obtained, using two calculation methods within the theoretical Johnson–Mehl–Avrami model. Each set of the results obtained is discussed regarding its agreement with previous experimental data. Finally, the phase at which the alloy crystallizes after the thermal process has been determined by X-ray diffraction.

1. Introduction

The knowledge of amorphous solids is now one of the most active fields of research in the physics of condensed materials [1]. The great interest in these materials is largely due to their ever increasing applications in modern technology. Their possibilities in the immediate future are huge, based on characteristic properties such as electronic excitation phenomena, chemical reactivity and inertia, superconductivity, etc.

An amorphous solid is a material which does not have the long-range order (periodicity) characteristic of crystalline materials, although it does have a certain local order in its bonds with first neighbours. "Amorphous" and "non-crystalline" are therefore synonymous terms, whereas "glass" is the non-crystalline material exhibiting a characteristic transition temperature [2] from the more energetic glass phase to the minimal energy crystalline phase.

The crystallization kinetics of amorphous alloys has been intensively studied using the classic Johnson–Mehl–Avrami (JMA) theoretical model [3]. Different authors have developed very diverse methods, based on the abovementioned JMA theoretical model, for calculating the kinetic parameters: activation energy, E, reaction order, n, and frequency factor, K_0 [4–9]. These methods are widely used in the literature, with varying results depending on the nature of the glassy alloys to which they are applied. In general, these developments are carried out under the hypothesis that the temperature is constant during the crystallization reaction, which means that the conclusions are strictly applicable only to experimental data obtained through isothermal techniques. However, these techniques are not always feasible, and it is sometimes more interesting to carry out differential scanning calorimetry (DSC) measurements by linear heating at a controlled rate β. It has been proved [10] that the application of results obtained under isothermal conditions to non-isothermal experimental data leads to satisfactory conclusions, with certain restrictions.

It has been observed that, given a fixed composition of alloy glass, the same set of kinetic parameters enables us to interpret the results obtained under both calorimetric conditions (isothermal and non-isothermal) [8]. It should also be interesting to find the sets of kinetic parameters supplied by different methods of analysis applied to experimental data obtained for a single alloy. In this work we will use two methods of analysis, which are described in section 2.

2. Theoretical background

As was mentioned above, the crystallization kinetics of amorphous alloys has been intensively studied using the classic JMA theoretical model [3,11,12]. The crystallized fraction, x, is

$$x = 1 - \exp[-(Kt)^n] , \quad (1)$$

where t is the time, n is the Avrami index or reaction order and K is defined as the reaction rate constant, which is usually assigned an Arrhenius temperature dependence

$$K = K_0 \exp(-E/RT) , \quad (2)$$

with E being the effective activation energy which describes the overall crystallization process and K_0 being the frequency factor.

In general, nucleation frequency and crystalline growth rate exhibit values far from Arrhenius-type behaviour [13,14]; however, for a sufficiently limited temperature range, such as the range of crystallization peaks in DSC experiments, both magnitudes can be considered to exhibit the said behaviour.

It is a well-known fact that eqs. (1) and (2) are used as the basis of nearly all DTA and DSC crystallization experiments but it must be noted that expression (1) can only be applied accurately in experiments carried out under isothermal conditions, for which it was deduced. However, this expression is often used for deducing relationships describing non-isothermal crystallization processes, because the values obtained for kinetic parameters are in good agreement with those determined through other methods. Kinetic parameters of eqs. (1) and (2) may be deduced through two different methods.

Method 1

This method [5] determines the crystallization rate by taking the first derivative of x relative to t in eq. (1) and imposing the condition of maximum $d^2x/dt^2 = 0$ to locate the maximum crystallization rate. In a satisfactory approximation, the following relationship is found

$$\ln(dx/dt)_p = \ln(0.37\, nK_0) - \frac{E}{R}\frac{1}{T_p} , \quad (3)$$

which shows that there is a linear relationship, whose slope gives us the activation energy of the process, between the experimental values of the logarithm of the crystallization rate and the inverse temperature, T_p (the magnitudes of which are measured at the instant when the maximum value is reached), corresponding to the different values of β (heating rate).

The other two kinetic parameters are obtained using the conditions

$$\frac{\beta E}{RK_p T_p^2} = 1 \quad \text{and} \quad (dx/dt)_p = 0.37\, nK_p , \quad (4)$$

which are also derived from the aforementioned mathematical reasoning.

Method 2

In this method, the crystallization rate is obtained by differentiating expression (1) with respect to time, bearing in mind the fact that in the non-isothermal process the reaction rate constant is a function of time through its Arrhenius temperature dependence [9] resulting in

$$\frac{dx}{dt} = n(Kt)^{n-1}\left(t\frac{dK}{dt} + K\right)(1-x) . \quad (5)$$

The maximum crystallization rate is found by making $d^2x/dt^2 = 0$, thus obtaining the relationship

$$(n-1)\left(t\frac{dK}{dt} + K\right)^2 + Kt\left(2\frac{dK}{dt} + t\frac{d^2K}{dt^2}\right) - n(Kt)^n\left(t\frac{dK}{dt} + K\right)^2 = 0 , \quad (6)$$

in which, by substituting the expressions for dK/dt and d^2K/dt^2 and introducing $T = T_0 + \beta t$, where T_0 is the initial temperature, we obtain the expression

$$\left(\frac{K_p(T_p - T_0)}{\beta}\right)^n = \frac{1}{n}\left[n - 1 + \left(\frac{E}{R(T_p - T_0)}\right)^2 \times \left(1 + \frac{E}{R(T_p - T_0)}\right)^{-2}\right] , \quad (7)$$

which relates the kinetic crystallization parameters E and n to the maximum values (denoted by subscript p) that can be determined experimentally, and which correspond to the maximum crystallization rate.

As in most crystallization processes $E/RT_p \gg 1$ (usually $E/RT_p \geqslant 25$), eq. (7) then becomes

$$\left(\frac{K_p(T_p - T_0)}{\beta}\right)^n \simeq 1 , \quad (8)$$

an expression from which it is deduced that the crystallized fraction for the maximum crystallization rate is 0.63, which, as may be observed, is independent of the heating rate and the reaction order. The logarithmic form of eq. (8) is

$$\ln \frac{T_p - T_0}{\beta} = \frac{E}{R} \frac{1}{T_p} - \ln K_0 , \quad (9)$$

which is a linear relationship, making it possible to calculate parameters E and K_0. At the same time, if the relationship $K_p(T_p - T_0)/\beta = 1$ is introduced into eq. (5), we obtain

$$n = \frac{(dx/dt)_p R T_p^2}{0.37 E K_p (T_p - T_0)} , \quad (10)$$

which makes it possible to calculate the reaction order or kinetic exponent n.

3. Experimental procedure

High-purity (99.999%) Sn, As and Se in appropriate atomic percentage proportions were introduced into a quartz glass ampoule (6 mm diameter). The contents of the ampoule (7 g total) were sealed at a pressure of 10^{-4} Torr and heated in a rotating furnace at around 1100 K for 72 h. The melt was quenched in air to obtain the glass. The glassy nature of the material was confirmed by X-ray diffraction in a Siemens D-500 diffractometer, showing an absence of the peaks that are characteristic of crystalline phases.

The thermal behaviour was investigated using a Rigaku thermoflex DSC instrument, to which an inert gas external installation was connected in order to ensure a constant He flow of 60 ml min^{-1} to purge the gases generated during the crystallization reaction, which, as is characteristic of chalcogenide materials, are damaging to the DSC sensory equipment. The temperature and energy calibrations of the instrument were performed using the well-known melting temperatures and melting enthalpies of high-purity In, Sn and Pb supplied with the instrument. The crystallization experiments were carried out through continuous heating at β rates of 4, 8, 16 and 32 K min^{-1}, and the masses used were kept within the range of 20 mg. The pulverized samples were crimped (but not hermetically sealed) into aluminum pans, and empty aluminum pans were used as reference.

With the aim of investigating the phase or phases at which the samples crystallize, diffractograms of the material crystallized during the DSC were obtained. The experiments were performed with a Philips diffractometer (type PW 1830). The patterns were run with Cu as target and Ni as filter ($\lambda = 0.1542$ nm) at 40 kV and 40 mA, with a scanning speed of $0.1^\circ\ s^{-1}$.

4. Results and discussion

The first property supplied by inspection of the thermograms obtained for the analyzed alloy is that their characteristic temperatures increase as the experimental heating rate β increases. The variation intervals of the magnitudes described by the thermograms for different heating rates are given in table 1, where T_g is the glass transition temperature, T_0 and T_p are the temperatures at which crystallization begins and that which corresponds to the maximum crystallization rate, respectively, and ΔT is the width of the peak. The crystallization enthalpies ΔH were also determined for the same heating rate at which the device was calibrated.

The area under the DSC curve is directly proportional to the total amount of alloy crystallized. The ratio between the ordinates and the total area of the peak gives the corresponding crystallization rates, which makes it possible to draw the curves of the exothermal peaks shown in fig. 1. It may be observed that the $(dx/dt)_p$ values increase in the same proportion as the heating rate, a property which has been widely discussed in the literature [5].

From the values of $(dx/dt)_p$ and T_p it is possible

Table 1
The characteristic temperatures and enthalpies of the crystallization process of alloy $Sn_{0.08}As_{0.26}Se_{0.66}$

Parameter	Values
T_g (K)	440–455
T_0 (K)	548–576
T_p (K)	591–629
ΔT (K)	78– 85
ΔH (mcal mg^{-1})	3.6

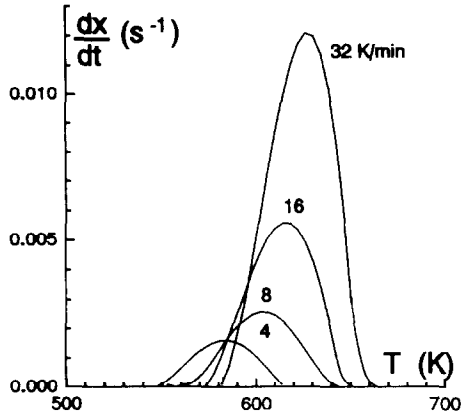

Fig. 1. Experimental curves of dx/dt versus T.

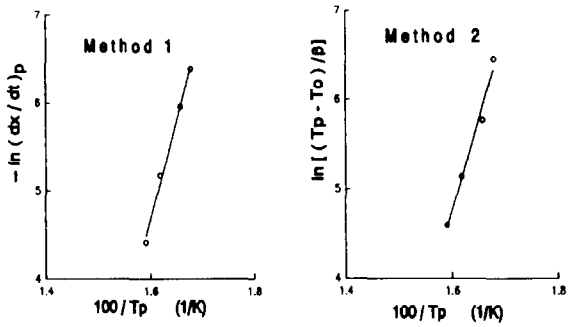

Fig. 2. Experimental plots and compromise straight lines for determining activation energy.

Table 2
Set of kinetic parameters calculated by the two methods

Method	E (kcal mol^{-1})	n	K_0 (s^{-1})
1	38.6	1.15	6.72×10^{11}
2	35.9	1.23	2.96×10^{10}

to draw the plots corresponding to eqs. (3) and (9) and the compromise straight lines the slopes of which give us the activation energies deduced by use of the equations predicted by methods 1 and 2. Fig. 2 shows the plots and compromise straight lines obtained by both methods, and table 2 shows the computed activation energy, E, values. By applying eqs. (4) and (10) it is possible to calculate the other two kinetic parameters, which are also shown in table 2.

A study of the results obtained by the aforementioned methods reveals slight differences. As to the activation energy and reaction order, the two values may be considered satisfactory, being within the margin of error accepted in the literature. The problem centres therefore on evaluating which of the two methods of calculation is the most suitable for finding the set of kinetic values; this may depend on the type of glassy material studied.

To do this, we propose to reconstruct the crystallization reaction, taking each set of kinetic parameters, according to eq. (3), and comparing them with the experimental one. Fig. 3 shows this reconstruction, representing crystallized fractions versus times, with the data corresponding to a heating rate of $\beta=8$ K min^{-1}.

In order to establish a criterion allowing us to decide on the most adequate calculation method, the mean-square deviation, σ, between the curves reconstructed with each set of kinetic parameters and the experimental curve was found for each heating rate. The parameters calculated through method 2 give the lowest values for the mean square deviation; $\sigma=0.20$ for method 1 and $\sigma=0.05$ for method 2.

The greater mathematical strictness used in method 2, which lies in the fact that in the two derivation steps for the crystallized fraction, the temperature dependence was taken into account and yet did not show any improvement in relation to the values given by method 1, which considers only the peak values of the experimental DSC curves.

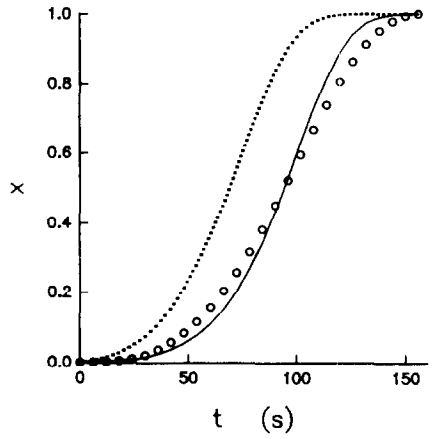

Fig. 3. Crystallized fraction versus t for the experimental values and for the curves corresponding to kinetic parameters calculated by the two methods for $\beta=8$ K min^{-1} ((○) experimental, (...) method 1, (—) method 2).

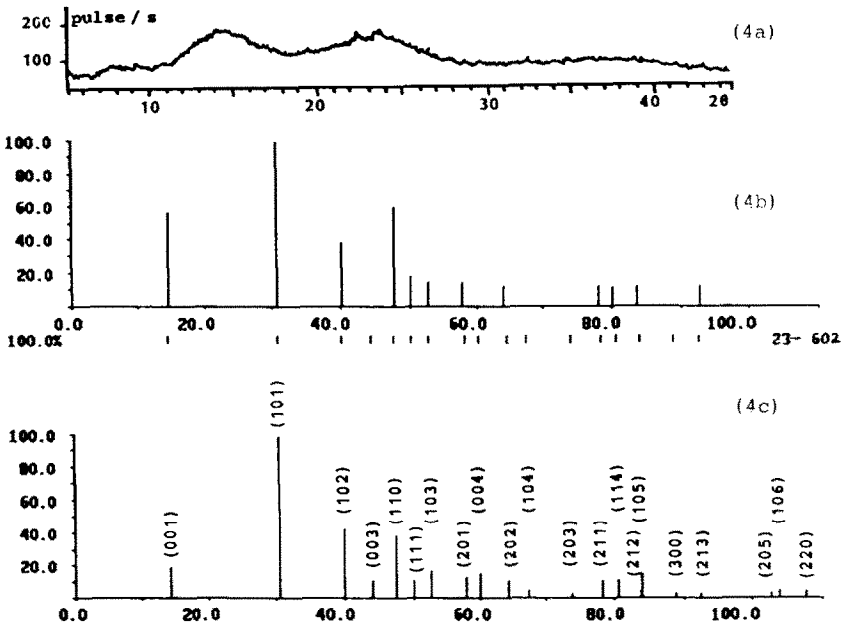

Fig. 4. (a) Diffractogram of amorphous alloy $Sn_{0.08}As_{0.26}Se_{0.66}$. (b) Diffraction peaks of alloy crystallized in DSC. (c) Diffraction peaks of single crystal $SnSe_2$ [15].

The comparison of the sigmoid curves shown in fig. 3 even leads us to the question whether the theoretical JMA model, as summarized in eqs. (1) and (2), equally describes the whole crystallization reaction.

In any case, the final comparison of the x versus t curves, reconstructed from the set of kinetic parameters, with the experimental curves, is suggested as a good procedure for verifying the agreement between the actual behaviour of the amorphous alloy when it crystallizes and the theoretical model describing this crystallization reaction.

X-ray diffractograms of the crystallized samples were obtained for each heating rate. For example, fig. 4 shows the diffraction peaks corresponding to the alloy crystallized in the DSC for $\beta = 32$ K min^{-1} together with the diffraction peaks corresponding to the single crystal $SnSe_2$, as well as the diffractogram of the amorphous alloy before crystallization.

All diffraction peaks of the different samples crystallized at rates $\beta = 4$, 8, 16 and 32 K min^{-1} can be assigned to a single phase of $SnSe_2$ with hexagonal symmetry [15] whose lattice parameters are $a = 0.381 \pm 0.002$ nm and $c = 0.614 \pm 0.005$ nm. Given the low concentration of Sn in the alloy, the amount of $SnSe_2$ crystal obtained in the process cannot be more than 25% of the total mass of the amorphous alloy, which may explain the low enthalpy value obtained.

Acknowledgement

The authors are grateful to Peter Asschert for his help in the translation of this paper into English, and to the Comisión Interministerial de Ciencia y Tecnología for their financial support (Project No. PB88-0463).

References

[1] R. Zallen, The physics of amorphous solids (Wiley, New York, 1983).
[2] S.R. Elliott, Physics of amorphous materials (Longman, London, 1984).
[3] M. Avrami, J. Chem. Phus. 7 (1939) 1103.
[4] Y.Q. Gao and W. Wang, J. Non-Cryst. Solids 81 (1986) 129.

[5] Y.Q. Gao, W. Wang, F.-D. Zheng and X. Liu, J. Non-Cryst. Solids 81 (1986) 135.
[6] J. Vázquez, R.A. Ligero, P. Villares and R. Jiménez-Garay, Thermochim. Acta 157 (1990) 181.
[7] R.A. Ligero, J. Vázquez, P. Villares and R. Jiménez Garay, Thermochim. Acta 162 (1990) 427.
[8] S. Suriñach, M.D. Baro, M.Y. Clavaquera-Mora and N. Clavaquera, J. Non-Cryst. Solids 58 (1983) 209.
[9] J.A. Augis and J.E. Bennett, J. Thermal Anal. 13 (1978) 283.
[10] T. Kemeny and L. Granasy, J. Non-Cryst. Solids 68 (1984) 193.
[11] W.A. Johnson and K.T. Mehl, Trans. Am. Inst. Mining. Met. Eng. 135 (1981) 315.
[12] M. Avrami, J. Chem. Phys. 8 (1940) 212.
[13] D. Turnball, Solid state physics, Vol. 3 (Academic Press, New York, 1956).
[14] J.W. Christian, The theory of transformations in metals and alloys, 2nd Ed. (Pergamon, Oxford, 1975).
[15] JCPDS, Powder Diffraction File, Card No. 23-602, Intern. Cent. Dif. Data (1988).